Identification of inhibitors of the immunosuppressive enzyme IL4I1

Marc Presset, Diana Djordjevic, Aurélie Dupont, Erwan Le Gall, Valérie Molinier-Frenkel, Flavia Castellano

Identification of inhibitors of the immunosuppressive enzyme IL4I1

Marc Presset[1], Diana Djordjevic[2,3], Aurélie Dupont[2,3], Erwan Le Gall[1], Valérie Molinier-Frenkel[2,3,4]*, and Flavia Castellano[2,3]*

[1] Electrochimie et Synthèse Organique, Université Paris Est, ICMPE (UMR 7182), CNRS, UPEC, 2 rue Henri Dunant, F-94320 Thiais, France ;

[2] INSERM, U955, Equipe 09, Créteil, France;

[3] Université Paris Est, Faculté de Médecine, Créteil, France;

[4] AP-HP, Hôpital H. Mondor - A. Chenevier, Laboratoire d'Immunologie, Créteil, France.

* Equal participation

Corresponding authors: Flavia Castellano and Valérie Molinier-Frenkel, INSERM U955, IMRB eq 09, Hôpital Henri Mondor, 51 av du Maréchal de Lattre de Tassigny, F-94010 Créteil cedex, France; flavia.castellano@inserm.fr, valerie.frenkel@inserm.fr, Tel: +33 1 49 813765, Fax: +33 1 49813566.

Running title: identification of IL4I1 inhibitors

Key words: immunosuppressive enzymes, cancer therapy, inhibitors, phenylalanine derivatives

1 INTRODUCTION

Recent advances in cancer immunotherapy have shown that limiting local or systemic cancer-related immunosuppression can result in long-lasting clinical responses. Amino-acid catabolizing enzymes reduce the availability of essential or semi-essential amino acids, while producing toxic products. Both effects result in impaired anti-tumor T-cell responses and the promotion of tumor growth [1]. Interleukin-4 Induced gene 1 (IL4I1) is a secreted L-phenylalanine oxidase expressed by antigen-presenting cells. *In vitro,* IL4I1 inhibits T-cell proliferation and cytokine production and facilitates the differentiation of naïve $CD4^+$ T cells into regulatory T cells, in part *via* its capacity to produce H_2O_2 and deplete phenylalanine from the T-cell microenvironment. IL4I1 is strongly detected in the tumor bed of most human tumor types and, in some cases, such as certain B cell lymphomas, it is expressed by the tumor cells themselves [2]. Local production of IL4I1 facilitates tumor growth in mouse models by inhibiting the proliferation and function of anti-tumor $CD8^+$ T cells and altering the balance of immune cells in the tumor microenvironment towards immunosuppressive populations [3 , 4]. Moreover, the localization and density of IL4I1-expressing cells correlates with pejorative clinical parameters and tend to predict shorter survival in patients suffering from melanoma [5]. A correlation between the presence of the IL4I1 protein or mRNA in the tumor and prognosis has also been observed in renal carcinoma, glioma (The Human Protein Atlas) [6], colon cancer [7] and breast cancer [8]. These data all suggest that therapeutic strategies aimed at inhibiting IL4I1 expression or activity in cancer patients may improve immune control of the tumor, without harming the host, as the absence of IL4I1 in KO mice does not appear to result in specific pathologies or premature death [9]. Targeting IL4I1 activity in the context of cancer treatment could thus become a new immunotherapy approach [10].

Phenylalanine (Phe) is the preferred substrate of IL4I1 catalytic activity. Our group has developed an approach for straightforward three-component reductive coupling between organic halides, amines, and aldehyde derivatives to produce α-branched amines [11],[12]. Here, we applied this method to synthesize 21 distinct phenylalanine derivatives and tested them, together with other 7 commercially available phenylalanine derivatives, as potential inhibitors of IL4I1 activity. Seven molecules inhibited IL4I1 enzymatic activity in the micromolar range and three of them were not toxic *in vitro*. One could reverse the negative effect of IL4I1 on T-cell proliferation in cell cultures. This work paves the way for the future development of clinically effective IL4I1 inhibitors.

2 METHODS

2.1 Chemical compounds (Cps)

Cp1 (ethyl 2-(4-methylpiperazin-1-yl)-3-phenylpropanoate), **Cp2** (ethyl propylphenylalaninate), **Cp3** (ethyl 3-(2,6-dichlorophenyl)-2-(piperidin-1-yl)propanoate), Cp**4** (ethyl 2-morpholino-3-phenylpropanoate), Cp**5** (ethyl 3-phenyl-2-(piperidin-1-yl)propanoate), **Cp6** (ethyl diethylphenylalaninate), **Cp7** (ethyl phenylphenylalaninate), Cp**8** (ethyl 2-(allylamino)-3-(3-(trifluoromethyl)phenyl)propanoate), and Cp**9** (ethyl 3-(4-cyanophenyl)-2-(phenylamino)propanoate) were prepared as described in [C. Haurena, E. Le Gall, S. Sengmany, T. Martens, M. Troupel, *J. Org. Chem.* **2010**, 75, 2645-2650]. Commercial phenylalanine derivatives : 3-(4-pyridyl)-L-alanine (Cp10), 1-methyl tryptophane (Cp11), benzoic acid, 3,4-dihydroxy-L-phenylalanine (Cp12), L-phenylalanine ethyl ester (Cp13), *N*-acetyl-phenylalanine (Cp14), 2-fluoro-phenylalanine (Cp15) were purchased from Sigma-Aldrich and used as received.

General procedure: In air, Zn (3.3 equiv) was placed in a round-bottom flask equipped with a stir bar and the flask closed with a septum and purged with Ar. CH_3CN (C = 0.25 M) and TFA (0.1 equiv) were added and the flask heated to reflux and then cooled to room temperature (RT). Benzyl halide (3.0 equiv) was added and the mixture was stirred at rt (for bromides) or at 60 °C (for chlorides) for 1 h. In air, a 2-necked round-bottom flask equipped with a stir bar, a condenser and an addition funnel was charged with ethyl glyoxylate (1.1 equiv) and the amine (1.0 equiv). The solution of organozinc halide in CH3CN was then added dropwise and the reaction was stirred at rt for 14 h. Then, the reaction mixture was poured into saturated aqueous NH_4Cl and the solution extracted twice with AcOEt. The combined organic layers were washed with brine, dried (Na_2SO_4) and evaporated to give the crude product, which was purified by an acid/base work-up, as described in the above-mentioned reference.

Cp2-SO4 was prepared as follows. H_2SO_4 (53 µL, 1.0 mmol, 0.5 equiv) was added to a solution of Cp**2** (0.49 g, 2.0 mmol) in anhydrous Et_2O (8 mL, C = 0.25 M) and the solution stirred at RT for 1 h. Then, the supernatant was removed and the paste dried to give the title compound as a sticky paste (333 mg, 50%). ^{1}H NMR (400 MHz, $CDCl_3$): δ 7.21 (s, 5H), 4.12 (dd, *J* = 10.1, 4.8 Hz, 1H), 4.04 (q, *J* = 7.1 Hz, 2H), 3.64 (dd, *J* = 13.4, 6.6 Hz, 1H), 3.26 (dd, *J* = 13.5, 10.5 Hz, 1H), 3.04-2.93 (m, 2H), 1.87-1.85 (m, 2H), 1.01 (t, *J* = 7.1 Hz, 3H), 0.87 (t, *J* = 7.4 Hz, 3H) [2 NH not detected]. HRMS (ESI/Q-TOF) m/z: $[M+H]^+$ Calcd for $C_{14}H_{25}NO_2S$ 236.1645; Found 236.1645.

Cp2-HCl was prepared as follows. A solution of **Cp2** (0.5 g, 2.1 mmol) in anhydrous Et_2O (20 mL, C = 0.1 M) was saturated with gaseous HCl (prepared by the addition of concentrated H_2SO_4 to NaCl) and the solution stirred at RT for 1 h. Then, the suspension was filtered on a fritted funnel and the solid dried to give the title compound as a white solid (0.57 g, 99%). ^{1}H NMR (400 MHz, MeOD): δ 7.37-7.31 (m, 5H), 4.33 (dd, *J* = 8.5, 5.4 Hz, 1H), 4.15 (q, *J* = 7.1 Hz, 2H), 3.49 (dd, *J* = 13.6, 5.1 Hz, 1H), 3.18 (dd, *J* = 13.6, 9.3 Hz, 1H), 3.10-3.00 (m, 2H), 1.84-1.78 (m, 2H), 1.10 (t, *J* = 7.1 Hz, 3H), 1.03 (t, *J* = 7.4 Hz, 3H) [2 NH not detected].

Cp2-TFA was prepared as follows. TFA (0.16 mL, 2.0 mmol, 1.0 equiv) was added to a solution of Cp2 (0.49 g, 2.0 mmol) in anhydrous Et_2O (8 mL, C = 0.25 M) and the solution stirred at RT for 1 h. Then, the suspension was filtered on a fritted funnel and the solid dried to give the title compound as a white solid (154 mg, 20%). ^{1}H NMR (400 MHz, $CDCl_3$): δ 7.31-7.28 (m, 3H), 7.21-7.19 (m, 2H), 4.13-4.07 (m, 3H), 3.44 (dd, *J* = 13.5, 4.8 Hz, 1H), 3.19 (dd, *J* = 13.4, 10.0 Hz, 1H), 3.08-3.01 (m, 1H), 2.98-2.91 (m, 1H), 1.83-1.78 (m, 2H), 1.08 (t, *J* = 7.1 Hz, 3H), 0.97 (t, *J* = 7.4 Hz, 3H) [2 NH not detected]. ^{13}C{^{1}H} NMR (100 MHz, $CDCl_3$): δ 168.1 (C), 162.3 (q, *J* = 35.8 Hz, C), 134.0 (C), 129.1 (2 CH), 128.8 (2 CH), 127.6 (CH), 62.3 (CH_2), 61.3 (CH), 48.4 (CH_2), 36.0 (CH_2), 19.6 (CH_2), 13.6 (CH_3), 11.0 (CH_3) [CF_3 not detected]. ^{19}F NMR (376 MHz, $CDCl_3$): δ -75.7 (s, 3F).

Cp7Bis (ethyl (2-(2-ethoxy-1-hydroxy-2-oxoethyl)phenyl)phenylalaninate) was isolated as a side-product of the preparation of **Cp7** during flash chromatography on a silica gel. ^{1}H NMR (400 MHz, $CDCl_3$): (2 diastereomers) δ 7.29 (s, 8H), 7.18-7.13 (m, 4H), 6,74 (dd, *J* = 7,3, 7.3 Hz, 2H), 6.60 (dd, *J* = 8.7, 8.7 Hz, 4H), 5.51 (s, 1H), 5.45 (s, 1H), 4.57 (br s, 2H), 4.42 (br s, 2H), 4.32-4.11 (m, 8H), 3.80 (br s, 1H), 3.73 (br s, 1H), 3.33-3.26 (m, 4H), 1.25-1.15 (m, 12H). ^{13}C{^{1}H} NMR (100 MHz, $CDCl_3$): (2 diastereomers) δ 173.8 (C), 173.8 (C), 173.5 (2 C), 146.6 (C), 146.6 (C), 137.3 (C), 137.2 (C), 135.5 (C), 135.2 (C), 130.8 (CH), 130.6 (CH), 129.2 (2 CH), 129.2 (2 CH), 128.7 (CH), 128.7 (CH), 127.8 (CH), 127.6 (CH), 127.5 (CH), 127.3 (CH), 118.5 (CH), 118.4 (CH), 113.7 (2 CH), 113.6 (2 CH), 70.4 (CH), 70.0 (CH), 62.2 (CH_2), 62.2 (CH_2), 61.3 (CH_2), 61.1 (CH_2), 58.4 (CH), 58.3 (CH), 35.7 (CH_2), 35.6 (CH_2), 14.0 (4 CH_3). HRMS (ESI/Q-TOF) m/z: $[M+H]^+$ Calcd for $C_{21}H_{26}NO_5$ 372.1805; Found 372.1811.

Cp2-pMe (ethyl 2-(propylamino)-3-(p-tolyl)propanoate): The general procedure performed with 4-methylbenzyl bromide (1.39 g, 7.5 mmol, 3.0 equiv), ethyl glyoxylate (0.64 mL, 50% in toluene, 2.75 mmol, 1.1 equiv) and *n*-propylamine (0.20 mL, 2.5 mmol, 1.0 equiv) afforded the title

compound (426 mg, 68%) as a yellow oil. ^{1}H NMR (400 MHz, $CDCl_3$): δ 7.05 (s, 4H), 4.07 (q, *J* = 7.1 Hz, 2H), 3.45 (t, *J* = 7.0 Hz, 1H), 2.89 (dd, *J* = 8.8, 7.1 Hz, 2H), 2.53 (ddd, *J* = 11.1, 8.1, 6.7 Hz, 1H), 2.42 (ddd, *J* = 11.1, 8.1, 6.2 Hz, 1H), 2.28 (s, 3H), 1.62 (br s, 1H), 1.47-1.40 (m, 2H), 1.13 (t, *J* = 7.0 Hz, 3H), 0.85 (t, *J* = 7.4 Hz, 3H). $^{13}C\{^{1}H\}$ NMR (100 MHz, $CDCl_3$): δ 174.5 (C), 135.8 (C), 134.0 (C), 128.8 (2 CH), 128.8 (2 CH), 62.9 (CH), 60.2 (CH_2), 49.8 (CH_2), 39.1 (CH_2), 23.0 (CH_2), 20.8 (CH_3), 13.9 (CH_3), 11.4 (CH_3). HRMS (ESI/Q-TOF) m/z: $[M+H]^+$ Calcd for $C_{15}H_{24}NO_2$ 250.1801; Found 250.1801.

Cp2-mMe (ethyl 2-(propylamino)-3-(m-tolyl)propanoate): The general procedure performed with 3-methylbenzyl bromide (1.0 mL, 7.5 mmol, 3.0 equiv), ethyl glyoxylate (0.64 mL, 50% in toluene, 2.75 mmol, 1.1 equiv) and *n*-propylamine (0.20 mL, 2.5 mmol, 1.0 equiv) afforded the title compound (432 mg, 69%) as a yellow oil. ^{1}H NMR (400 MHz, $CDCl_3$): δ 7.15 (dd, *J* = 7.4, 7.4 Hz, 1H), 7.02-6.97 (m, 3H), 4.09 (q, *J* = 7.0 Hz, 2H), 3.48 (t, *J* = 7.0 Hz, 1H), 2.96-2.84 (m, 2H), 2.57-2.51 (m, 1H), 2.43 (ddd, *J* = 11.1, 8.1, 6.3 Hz, 1H), 2.31 (s, 3H), 1.64 (br s, 1H), 1.49-1.42 (m, 2H), 1.14 (t, *J* = 7.0 Hz, 3H), 0.86 (t, *J* = 7.4 Hz, 3H). $^{13}C\{^{1}H\}$ NMR (100 MHz, $CDCl_3$): δ 174.7 (C), 137.7 (C), 137.2 (C), 129.9 (CH), 128.1 (CH), 127.2 (CH), 126.1 (CH), 63.0 (CH), 60.3 (CH_2), 49.9 (CH_2), 39.6 (CH_2), 23.1 (CH_2), 21.2 (CH_3), 14.1 (CH_3), 11.5 (CH_3). HRMS (ESI/Q-TOF) m/z: $[M+H]^+$ Calcd for $C_{15}H_{24}NO_2$ 250.1801; Found 250.1802.

Cp2-sulfamide (ethyl N-(methylsulfonyl)-N-propylphenylalaninate) was prepared as follows. Triethylamine (0.3 mL, 2.0 mmol, 2.0 equiv) and mesyl chloride (0.1 mL, 1.1 mmol, 1.1 equiv) was added to a solution of **Cp2** (235 mg, 1.0 mmol) in CH_2Cl_2 (2 mL) at 0 °C under Ar and the reaction stirred at 0°C for 2 h. Then, the reaction mixture was poured into saturated aqueous NH_4Cl (10 mL) and extracted twice with CH_2Cl_2 (2x10 mL). The combined organic layers were dried (Na_2SO_4) and evaporated. Purification of the residue by flash chromatography gave the title compound as a colorless oil (176 mg, 56%). ^{1}H NMR (400 MHz, $CDCl_3$): δ 7.32-7.25 (m, 5H), 4.74 (t, *J* = 7.4 Hz, 1H), 4.19 (q, *J* = 7.0 Hz, 2H), 3.38 (dd, *J* = 14.1, 7.4 Hz, 1H), 3.28-3.20 (m, 1H), 3.13 – 3.03 (m, 2H), 2.73 (s, 3H), 1.691.58 (m, 2H), 1.26 (t, *J* = 7.0 Hz, 3H), 0.89 (t, *J* = 7.4 Hz, 3H). $^{13}C\{^{1}H\}$ NMR (100 MHz, $CDCl_3$): δ 170.8 (C), 137.1 (C), 129.3 (2 CH), 128.6 (2 CH), 127.0 (CH), 61.8 (CH), 61.7 (CH_2), 48.0 (CH_2), 39.9 (CH_3), 37.0 (CH_2), 23.4 (CH_2), 14.1 (CH_3), 11.4 (CH_3). HRMS (ESI/Q-TOF) m/z: $[M+H]^+$ Calcd for $C_{15}H_{24}NO_4S$ 314.1420; Found 314.1417.

Cp2-sulfamic acid (1-ethoxy-1-oxo-3-phenylpropan-2-yl)(propyl)sulfamic acid) was prepared as follows. Chlorosulfonic acid (25 µL, 0.38 mmol, 1.1 equiv) was added to a solution of **Cp2** (82 mg,

0.35 mmol) in CH_2Cl_2 (2 mL) at 0°C under Ar and the reaction stirred at 0°C for 2 h. Then, the reaction mixture was evaporated and Et_2O (10 mL) added. The resulting mixture was stirred overnight at RT and the suspension filtered on a fritted funnel and the solid dried to give the title compound (89 mg, 80%) as a white solid. ^{1}H NMR (400 MHz, $CDCl_3$): δ 8.96 (s, 1H), 7.29-7.24 (m, 5H), 4.19 (br s, 1H), 4.07 (q, *J* = 7.1 Hz, 2H), 3.63 (dd, *J* = 13.1, 4.6 Hz, 1H), 3.29 – 3.23 (m, 1H), 3.11 (br s, 1H), 2.98 (br s, 1H), 1.93-1.86 (m, 2H), 1.03 (t, *J* = 7.1 Hz, 3H), 0.93 (t, *J* = 7.3 Hz, 3H). ^{13}C{^{1}H} NMR (100 MHz, $CDCl_3$): δ 168.2 (C), 134.2 (C), 129.5 (2 CH), 128.8 (2 CH), 127.6 (CH), 62.6 (CH), 61.9 (CH_2), 49.4 (CH_2), 36.4 (CH_2), 19.6 (CH_2), 13.8 (CH_3), 11.0 (CH_3). HRMS (ESI/Q-TOF) m/z: $[M–H]^-$ Calcd for $C_{14}H_{20}NO_5S$ 314.1067; Found 314.1066.

Cp16 (ethyl 3-(2,6-dichlorophenyl)-2-(diethylamino)propanoate): The general procedure performed with 2,6-dichlorobenzyl bromide (3.6 g, 15 mmol, 3.0 equiv), ethyl glyoxylate (1.3 mL, 50% in toluene, 5.5 mmol, 1.1 equiv) and diethylamine (0.52 mL, 5 mmol, 1.0 equiv) afforded the title compound (1.064 g, 67%) as a yellow oil. ^{1}H NMR (400 MHz, $CDCl_3$): δ 7.25 d, *J* = 7.9 Hz, 2H), 7.06 (t, *J* = 7.9 Hz, 1H), 4.11 (q, *J* = 7.0, 2H), 3.92 (t, *J* = 7.6 Hz, 1H), 3.39–3.23 (m, 2H), 2.79–2.74 (m, 2H), 2.58–2.53 (m, 2H), 1.18 (t, *J* = 7.0 Hz, 3H), 0.93 (t, *J* = 6.9 Hz, 6H). ^{13}C{^{1}H} NMR (100 MHz, $CDCl_3$): δ 172.6 (C), 136.0 (2 C), 135.2 (C), 128.0 (2 CH), 127.8 (CH), 60.7 (CH_2), 60.2 (CH), 44.3 (2 CH_2), 31.5 (CH_2) 14.3 (CH_3), 13.8 (2 CH_3). HRMS (ESI/Q-TOF) m/z: $[M+H]^+$ Calcd for $C_{15}H_{22}Cl_2NO_2$ 318.1022; Found 318.1020.

Cp17 (ethyl diethylphenylalaninate): The general procedure performed with benzyl chloride (1.9 mL, 15 mmol, 3.0 equiv), ethyl glyoxylate (1.3 mL, 50% in toluene, 5.5 mmol, 1.1 equiv) and diethylamine (0.52 mL, 5 mmol, 1.0 equiv) afforded the title compound (0.82 g, 65%) as a yellow oil. ^{1}H NMR (400 MHz, $CDCl_3$): δ 7.36–7.11 (m, 5H), 4.10 (ddd, *J* = 6.8, 4.5, 2.1 Hz, 2H), 3.68–3.59 (m, 1H), 3.15–3.04 (m, 1H), 2.91 (dd, *J* = 13.4, 6.2 Hz, 1H), 2.81 (ddd, *J* = 14.5, 8.2, 6.4 Hz, 2H), 2.57 (ddd, *J* = 13.3, 6.9, 1.9 Hz, 2H), 1.18 (t, *J* = 7.2 Hz, 3H), 1.05 (t, *J* = 7.1 Hz, 5H). ^{13}C{^{1}H} NMR (100 MHz, $CDCl_3$): δ 172.6 (C), 138.8 (C), 129.3 (2 CH), 128.2 (2 CH), 126.2 (CH), 65.0(CH), 60.0 (CH_2), 44.5 (2 CH_2), 36.4 (CH_2), 14.3 (CH_3), 13.8(2 CH_3). HRMS (ESI/Q-TOF) m/z: $[M+H]^+$ Calcd for $C_{15}H_{24}NO_2$ 250.1801; Found 250.1800.

Cp18 (ethyl 3-(2,6-dichlorophenyl)-2-(propylamino)propanoate): The general procedure performed with 2,6-dichlorobenzyl bromide (3.6 g, 15 mmol, 3.0 equiv), ethyl glyoxylate (1.3 mL, 50% in toluene, 5.5 mmol, 1.1 equiv) and *n*-propylamine (0.4 mL, 5 mmol, 1.0 equiv) afforded the title compound (0.58 g, 38%) as a yellow oil. ^{1}H NMR (400 MHz, $CDCl_3$): δ 7.25 (d, *J* = 7.8 Hz, 2H), 7.07 (t, *J*

= 7.8 Hz, 1H), 4.08 (q, *J* = 7.4 Hz, 2H), 3.64–3.61 (m, 1H), 3.26–3.22 (m, 2H), 2.60–2.35 (m, 2H), 1.71 (br s, 1H), 1.50–1.35 (m, 2H), 1.11–1.08 (m, 3H), 0.84 (t, *J* = 9.4 Hz, 3H). $^{13}C\{^{1}H\}$ NMR (100 MHz, $CDCl_3$): δ 174.5 (C), 136.0 (2 C), 134.3 (C), 128.1 (CH), 128.1 (2 CH), 60.8 (CH_2), 60.0 (CH), 49.9 (CH_2), 35.2 (CH_2), 23.2 (CH_2), 14.0 (CH_3), 11.6 (CH_3). HRMS (ESI/Q-TOF) m/z: $[M+H]^+$ Calcd for $C_{14}H_{20}Cl_2NO_2$ 304.0865; Found 304.0865.

Cp19 (ethyl 3-phenyl-2-(piperidin-1-yl)propanoate): The general procedure performed with benzyl chloride (1.9 mL, 15 mmol, 3.0 equiv), ethyl glyoxylate (1.3 mL, 50% in toluene, 5.5 mmol, 1.1 equiv) and piperidine (0.5 mL, 5 mmol, 1.0 equiv) afforded the title compound (0.78 g, 59%) as a yellow oil. ^{1}H NMR (400 MHz, $CDCl_3$): δ 7.27–7.21 (m, 5H), 4.08–4.06 (m, 2H), 3.42 (dd, *J* = 9.9, 5.4 Hz, 1H), 3.12–3.06 (m, 1H), 2.97 (dd, *J* = 13.1, 4.9 Hz, 1H), 2.75–2.55 (m, 4H), 1.70–1.35 (m, 6H), 1.13 (t, *J* = 7.1 Hz, 3H). $^{13}C\{^{1}H\}$ NMR (100 MHz, $CDCl_3$): δ 171.4 (C), 138.4 (C), 129.3 (2 CH), 128.2 (2 CH), 126.3 (CH), 70.4 (CH), 59.9 (CH_2), 51.1 (CH_2), 35.9 (CH_2), 26.4 (3 CH_2), 24.6 (CH_2), 14.4 (CH_3). HRMS (ESI/Q-TOF) m/z: $[M+H]^+$ Calcd for $C_{16}H_{24}NO_2$ 262.1801; Found 262.1800.

Cp20 (methyl propylphenylalaninate) was prepared as follows. A solution of **Cp2** (235 mg, 1.0 mmol) and $Sc(OTf)_3$ (98 mg, 0.2 mmol, 0.2 equiv) in CH_3OH (10 mL) was heated under reflux for 18 h. Then, the reaction mixture was evaporated. Purification of the residue by flash chromatography gave the title compound as a yellow oil (176 mg, 79%). ^{1}H NMR (400 MHz, $CDCl_3$): δ 7.30–7.18 (m, 5H), 3.64 (s, 3H), 3.54 (t, *J* = 6.9 Hz, 1H), 2.97 (t, *J* = 7.0 Hz, 2H), 2.59–2.42 (m, 2H), 1.49–1.46 (m, 3H), 0.88 (t, *J* = 7.3 Hz, 3H). $^{13}C\{^{1}H\}$ NMR (100 MHz, $CDCl_3$): δ 175.1 (C), 137.2 (C), 129.0 (2 CH), 128.3 (2 CH), 126.6 (CH), 63.0 (CH), 51.5 (CH_3), 50.0 (CH_2), 39.6 (CH_2), 23.1 (CH_2), 11.5 (CH_3). HRMS (ESI/Q-TOF) m/z: $[M+H]^+$ Calcd for $C_{13}H_{20}NO_2$ 222.1488; Found 222.1487.

2.2 Sample preparation for in vitro assays

Stock solutions to be used for the enzymatic and cellular tests were prepared by suspending the compounds in DMSO at a concentration of 100 mM. Working solutions of the compounds were diluted in DMSO and stored at -20°C. Potential inhibitors were added at a 1:1000 dilution to the enzyme solution or culture medium.

2.3 Cells

Peripheral blood mononuclear cells (PBMCs), obtained from healthy donors by cytapheresis, were provided by the Etablissement Français du Sang (EFS) and separated using Unisep tubes filled with lymphocyte-separation medium (EuroBio, France). The Jurkat T cell line and human PBMCs were

cultivated in RPMI 1640 medium containing 10% fetal calf serum, 50 U/mL penicillin, and 50 µg/mL streptomycin. For measures of cell growth, Jurkat cells were seeded at 0.1 x 10^6/mL in a 24-well plate and counted on days 1, 2, 3, and 6 in disposable Fast-read 10 chambers after dilution in Trypan blue. THP1 and THP1 cells stably expressing IL4I1 (THP1-IL4I1) have been described previously [13] and were used in proliferation experiments after irradiation at 200 Gy.

2.4 Determination of Ki.

Recombinant human IL4I1 (from R&D Systems, Inc) was diluted in PBS at 100 ng/mL and pre-incubated for 30 min with various amounts of each inhibitor dissolved in DMSO (50, 25, and 2.5 µM) or DMSO as a control. The activity was tested in the presence of various amounts of substrate (0.25, 0.5, 1, 2, or 10 mM phenylalanine) using the fluorometric IL4I1 assay described by Carbonnelle-Puscian et al. [2]. The Ki for competitive inhibition was calculated using Graph Pad Prism software.

2.5 Metabolism-based cell proliferation assay.

Jurkat cells were seeded at 0.1 x 10^6/mL in a 96-well flat-bottom plate and incubated at 37°C in 5% CO_2. At successive time points, cells were centrifuged, the medium removed, and CellTiter 96® Non-Radioactive Cell Proliferation Assay reagent (Promega) added. The cells were then incubated an additional 4 h before measuring the optical density at 570 nm in a plate reader (BMG Labtech Fluostar Optima).

2.6 Apoptosis assay.

Cells were seeded at 5 x 10^5/mL in 24-well plates, with or without the compounds at 100 µM or 10 µM etoposide (VP16) as a positive control, and incubated at 37°C for 24 h. Cells were then fixed and permeabilized using cytox/cytoperm solution (BD Bioscience), followed by the addition of anti-activated caspase 3-AlexaFluor 647 (Rabbit anti-active Caspase 3 clone C92-605, BD Pharmingen). Data acquisition was performed on a Cyan ADP LX7 (Beckman Coulter) or Fortessa X20 (BD Bioscience), followed by analysis using Flowjo 10 software.

2.7 Flow cytometry analysis of cell proliferation.

Jurkat cells and PBMCs were labeled with 2 µM Cell Proliferation Dye (CPD) eFluor670 (Thermo Fisher) for 10 min at 37°C. Each compound or control DMSO was added to the cells before seeding them at 2 x 10^5/well in 96-well U-shaped plates. PBMCs were stimulated in plates pre-coated overnight with an anti-CD3 antibody (clone OKT3, eBioscience) at 0.5 µg/mL in PBS. Cells were collected on day 0, 3, and 6 for fluorescence acquisition using a Cyan ADP LX7 (Beckman Coulter).

The reversion of the effect of IL4I1 on T cell proliferation was tested by incubating PBMCs labeled with CPD (2 x 10^5/well) with irradiated THP1 or THP1-IL4I1 cells (2.5 x 10^5/well) in the presence of various concentrations of Cp2-SO4 dissolved in DMSO (100, 200, or 400 μM) or the equivalent volume of DMSO. Proliferation was induced by the addition of soluble OKT3 (20 ng/mL). Cells were collected on day 5 for flow cytometry acquisition on a Fortessa X20 (BD Bioscience). FlowJo 10 software was used for all data analyses and the calculation of proliferation and expansion indices. Statistical analysis (paired Student t-test) was performed using Prism 6.0.

3 RESULTS

3.1 Synthesis of the phenylalanine derivatives

IL4I1 is an immunosuppressive enzyme and the ability to control its enzymatic activity could be beneficial in situations in which its ectopic or deregulated activity limits the immune response, as in cancer. We generated potential inhibitors of IL4I1 by modifying the backbone of its preferential substrate, phenylalanine, using an expedient three-component Mannich-type reaction using aldehyde derivatives of organic halides to produce α-branched amines. We also tested 7 commercially available phenylalanine derivatives. The various compounds tested and their structures are shown in **Table I.**

Compound structure	Compound number	Inhibitory activity and KI (μM)
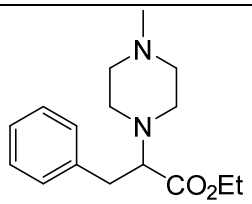	1	N.I.
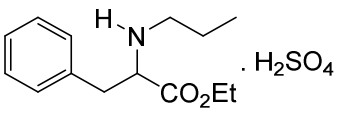	2-SO4	21.2 ± 5.9
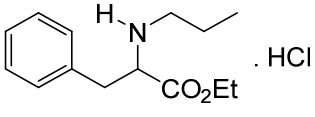	2-HCl	N.I.
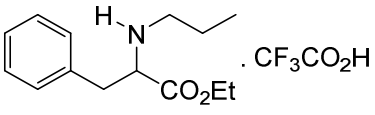	2-TFA	N.I.
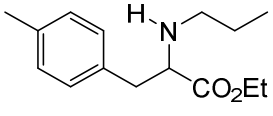	2-pMe	N.I.

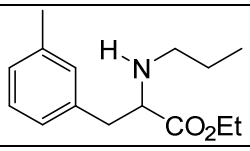	2-mMe	N.I.
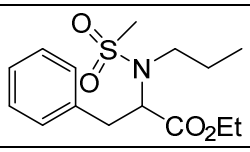	2-sulfamide	N.I.
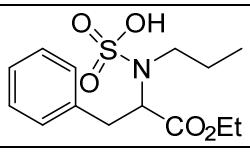	2-sulfamic acid	N.I.
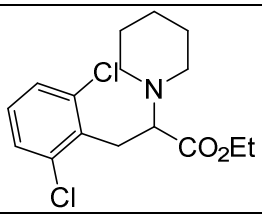	3	9.8 ± 4.6
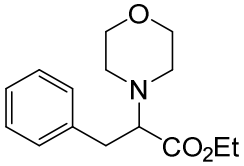	4	N.I.
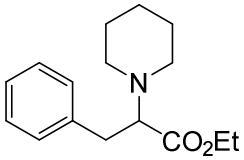	5	N.I.
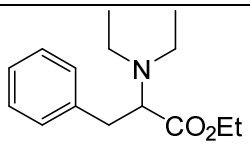	6	102.0 ± 29.7
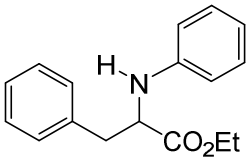	7	26.8 ± 6.9
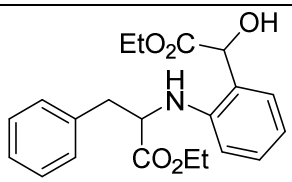	7bis	24.8 ± 12.2
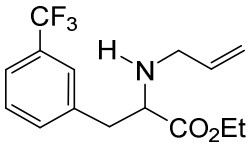	8	N.I.
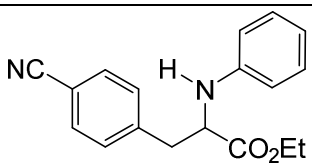	9	N.I.
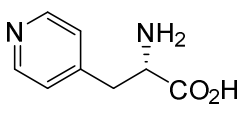	10	2800 ± 310

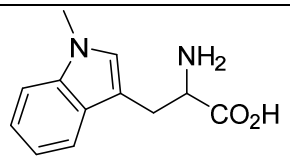	11	N.I.
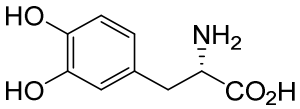	12	N.I.
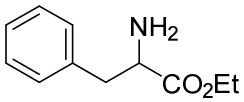	13	3100± 560
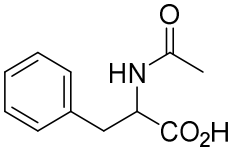	14	2100 ± 696
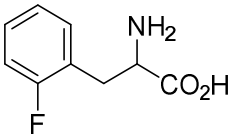	15	N.I.
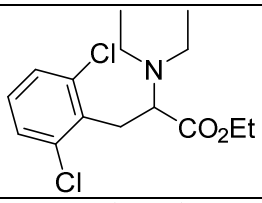	16	N.I.
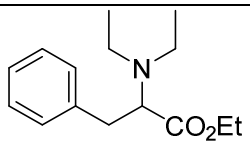	17	N.I.
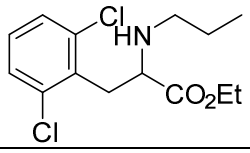	18	49.9 ± 20.9
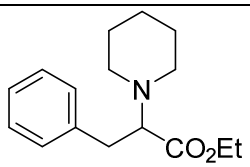	19	333.9 ± 198.0
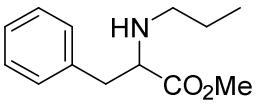	20	1320

Table 1 – Structure of the phenylalanine derivatives tested as inhibitors of IL4I1. Compounds are listed with numbers. Ki of inhibition were obtained using Graph Pad Prism software and using 3 different concentrations of each compound (50, 25 and 2.5 µM) in the modified enzymatic test described by Carbonelle-Puscian [14] Tests were performed 3 times for Cp1 to Cp17, two times for Cp18 and Cp19 and once for Cp20. N. I. means no inhibition. Values are reported in µM ±S.D.

3.2 Characterization of the IL4I1 inhibitory capacity of the phenylalanine derivatives

We first determined the inhibitory properties of the 21 phenylalanine derivatives synthetized using our method and 7 commercially available compounds on the enzymatic activity of IL4I1. Purified recombinant human IL4I1 enzyme was pre-incubated for 30 min with decreasing amounts of each inhibitor and the IL4I1 enzymatic activity tested in the presence of variable amounts of substrate to perform a Michaelis-Menten reaction, using a variation of the fluorometric method described by Carbonnelle-Puscian [2]. Most compounds, such as Cp4, Cp5, Cp8, Cp9, Cp11, Cp15, Cp16, Cp17 and all Cp2 derivatives except Cp2-SO4, did not interfere with IL4I1 activity. Cp1, which is modified on the amino group by an aromatic $CH_2CH_2N(CH_3)CH_2CH_2$ group, and the di-phenyl-hydroxy-phenylalanine did not block the activity and behaved as a slightly more efficient substrate of IL4I1 than phenylalanine (data not shown). Benzoic acid has been previously suggested as an inhibitor of IL4I1 [15]. We indeed measured diminished IL4I1 activities in the presence of benzoic acid but this was due to its effect on the peroxidase used in the indirect enzymatic test to measure H_2O_2 production. Seven compounds (Cp2-SO4, Cp3, Cp6, Cp7, Cp7Bis, Cp18 and Cp19) showed inhibitory activity in the micromolar range, while Cp10, Cp13, Cp14 and Cp20 inhibited IL4I1 activity in the millimolar range, although Cp14 later became a substrate for IL4I1. The competitive inhibition of human IL4I1 activity and their Kis are reported in **Figure 1** for Cp2-SO4, Cp3, Cp6, Cp7 and Cp7Bis and in **Table 1** for all compound tested, respectively. Amongst the most effective compounds, Cp6, Cp18 and Cp19 displayed the weakest inhibitory activity. Cp2-SO4, Cp7, and Cp7Bis showed a similar inhibitory capacity, with Ki of 21.26 ± 5.9, 26.89 ± 6.91, and 24.82 ± 12.1 µM, respectively. Cp3, characterized by two Cl groups on the aromatic ring of phenylalanine and a $CH_2CH_2CH_2CH_2CH_2$ group on the lateral chain, showed the strongest inhibitory capacity with a Ki of 9.8 ± 4.6 µM. Some of the Cps, although active against the human enzyme, did not inhibit mouse IL4I1 (data not shown).

3.3 Cp2-SO4 and Cp6 are not toxic

We next sought to verify whether the active inhibitors interfere with cell viability and proliferation (**Figures 2, 3, & 4**). Since IL4I1 acts on T lymphocytes, we first chose the human T-cell line Jurkat for our tests. Cells were cultivated in the presence of 100 µM of each inhibitor and compared to cells to which an equivalent volume of DMSO, the vehicle of the inhibitors (1:1000 maximum), had been added. We initially counted the viable cells at various time points to generate growth curves (**Figure 2A)**. Compounds such as Cp10 were extremely toxic even at doses largely inferior to the Ki values (data not shown) excluding them from any possible consideration and further work in cellular systems. Cp3 and Cp7 significantly slowed the growth of Jurkat cells, as early

as one day after the beginning of the culture, with no more viable cells detectable by day 6. On the contrary, Cp2-SO4, Cp6, and Cp7Bis did not substantially decrease the growth of Jurkat cells, even after six days. We confirmed these results using a metabolism-based cell proliferation assay: while Cp3 and Cp7 strongly limited Jurkat cell proliferation, Cp2-SO4 and Cp6 had no effect (**Figure 2B**). Finally, we analyzed the effect of Cp2-SO4 and Cp6 on the proliferation of both Jurkat cells (**Figure 3A**) and primary human T cells stimulated with an anti-CD3 antibody (**Figure 3B**). The cells were labeled with a fluorescent cell-proliferation dye (CPD) on day 0 and the dilution of the dye induced by cell division was measured by flow cytometry during the next several days. As expected, the two compounds had no effect on the proliferation of Jurkat cells relative to cells treated with DMSO. Interestingly, the proliferation of primary T-cells was also not affected, as established by calculation of the expansion and proliferation indices (**Figure 3C**).

Thus, the candidate inhibitors Cp2-SO4 and Cp6 did not inhibit cell proliferation. However, they may still induce apoptotic cell death. We evaluated this possibility by first incubating Jurkat cells overnight with various compounds, including Cp2-SO4, Cp6, Cp7Bis or etoposide (VP16, a clinical chemotherapy drug known for its proapoptotic properties [16]), as a positive control. We then measured the appearance of the cleaved form of caspase 3, which results from its activation during the early stages of apoptosis (**Figure 4**). Cp3 and Cp7 both induced the activation of caspase 3 in Jurkat cells, with Cp3 displaying a proapoptotic effect equivalent to that of VP16. In contrast, neither Cp2-SO4 nor Cp6 and Cp7Bis induced significant caspase 3 activation, *i.e.* above the levels detected in DMSO-treated control Jurkat cells. Cp2-SO4 and Cp6 also did not induce the apoptosis of primary lymphocytes. Thus, our data suggest that the phenylalanine derivatives Cp2-SO4 and Cp6 are non-toxic *in vitro* for human primary cells.

3.4 Reversion of the inhibitory effect of IL4I1 by Cp2-SO4.

IL4I1 is an immunosuppressive enzyme, which mainly functions as an inhibitor of T-cell proliferation. We thus decided to test whether Cp2-SO4 can reverse the antiproliferative effect of IL4I1 on T cells. We stimulated PBMCs with an anti-CD3 antibody, with or without IL4I1, using the THP1 and THP1-IL4I1 cell lines as described by Marquet et al. [13]. As expected, polyclonal T-cell stimulation was inhibited in the presence of IL4I1 (**Figure 5A**). Both the mean division number, evaluated by the proliferation index (**Figure 5B**), and the total population amplification, evaluated by the expansion index (**Figure 5C**), were affected. This inhibition was reversed in a dose dependent manner by the addition of Cp2-SO4. A proliferation level similar to that of PBMCs stimulated without IL4I1 was obtained with doses of the inhibitor of 200 and 400 µM. Thus, our data identify the first non-toxic

IL4I1 inhibitor that is effective in the micromolar range to reverse IL4I1 inhibitory effect and that could be used to block IL4I1-induced immunosuppression.

4 DISCUSSION

IL4I1 has been implicated in tumor escape from the immune response and represents a promising candidate for cancer immunotherapy. No specific inhibitors have been described for this enzyme to date. Here, we characterize *in vitro*, for the first time, small phenylalanine derivatives with IL4I1 inhibitory activity without an apparent toxic effect on human cells. One of the compounds can reverse the blocking effect of IL4I1 on T cell proliferation, thus displaying the expected biological effect.

Among the 28 molecules tested, only 7 showed inhibitory activity in the micromolar range. Their comparison allowed us to identify several chemical features that are important for the inhibitory effect and those to avoid reducing cell toxicity. Indeed, all compounds, except Cp3 and Cp18, which are modified on the aromatic group of phenylalanine (*i.e.* Cp8, Cp9, Cp2-pMe, and Cp2-mMe) did not show inhibitory activity, suggesting that the aromatic group may be important to enter the catalytic groove of IL4I1. IL4I1 is an L-amino acid oxidase similar to those found in snake venom [17]. Many of these enzymes have a strong preference for hydrophobic amino acids which perfectly suit the hydrophobic binding pocket in their catalytic cavity, as shown by crystallization studies. Substitutions at the phenylalanine ring may create steric hindrance at the active site [18] and thus interfere with the capacity of the inhibitor to compete with the natural substrate. An exception appears to be the presence of Cl groups on the aromatic ring. Indeed, these groups seem to confer strong inhibitory activity to Cp3, which otherwise shares the same structure with the non-active Cp5.

Surprisingly, Cp2-SO4 showed an inhibitory activity while Cp2 associated with different counter ions was not effective. One hypothesis is that the counter ion can change the solubility of the compound or its stability, thus facilitating or prolonging its inhibitory activity. This would be consistent with recently reported data on two different salts of an inhibitor of the human β tryptase [19]. Alternatively, the counter ion may directly participate to the inhibitory effect. This second hypothesis is supported by the structural studies of Pawelek of the L-Amino acid oxidase from *Calloselasma rhodostoma* which is highly homologous to IL4I1 [20]. Indeed, the α carbon atom of the phenylalanine substrate forms a strong salt bridge interaction with the guanidinium group of

Arg90 (equivalent to Arg97 in human IL4I1) of the catalytic site. Thus, the H_2SO_4 counter ion may be more efficient in competing for this interaction than the others we tested.

We tested the toxicity of the active molecules *in vitro* on a human T-cell line and primary human PBMCs. The most active compound, Cp3, showed strong toxicity. Cp7 was also toxic, as seen in both cell proliferation and the induction of apoptosis. Modification of the R3 position by a C_6H_5 group in the Cp7Bis molecule reduced this toxicity to values comparable to the control, while almost keeping the same Ki. These observations will be important for future improvements of the active compounds.

We tested one of the nontoxic active compounds, Cp2-SO4, for its ability to reverse the immunosuppressive action of IL4I1 *in vitro*. Indeed, the compound was able to restore T-cell proliferation, even with a Ki that is only in the micromolar range. This suggests that improving the backbone of any of our nontoxic compounds to more strongly inhibit the enzymatic activity of IL4I1 could be a valid approach to develop clinically amenable anticancer drugs.

5 CONCLUSION

In this work we have identified easily synthesizable phenylalanine derivatives endowed with IL4I1 inhibitory activity. Even if the non-toxic Cp2-SO4 had a Ki in the micromolar range, it was able to reverse IL4I1 inhibitory effect *in vitro* on human T cells. Since IL4I1 plays a role in tumor escape from the immune system, such inhibitors may be envisioned as a basis for future development of anti-cancer drugs.

6 AKNOWLEDGEMENTS

This work was conducted with the support of Bristol-Myers Squibb Foundation for Research in Immuno-Oncology, with the support of the Institut National du Cancer grant PLBIO18-255, and a pre-maturation grant from SATT-idf-Innov/UPEC/IMRB/IPCME. We thank Allan Thiolat for help in cell irradiation. This work has been revised by a professional English editing company (Alex Edelman & associates).

7 CONFLICT OF INTEREST

The authors declare no commercial or financial conflict of interest.

8 AUTHORS' CONTRIBUTIONS

Chemical synthesis: Marc Presset, Erwan Le Gall

Conception, design and supervision: Flavia Castellano and Valérie Molinier-Frenkel

Development of methodology: Flavia Castellano

Acquisition of the data: Aurelié Dupont, Diana Djordjevic, Flavia Castellano

Analysis and interpretation of data: Flavia Castellano and Valérie Molinier-Frenkel

Writing, review, and/or revision of the manuscript: Valérie Molinier-Frenkel, Erwan Le Gall, Marc Presset and Flavia Castellano

9 FIGURE LEGENDS

Figure 1. Michaelis-Menten plots of the molecules tested. Serial dilutions of the compounds (2.5, 25, and 50 µM) dissolved in DMSO were tested on the activity of a 100 ng/mL solution of recombinant human IL4I1 using various concentrations of the enzyme substrate. Controls (0 µM) contained an equal volume (1:1000) of DMSO. The data shown are mean ± SEM of two to four independent experiments.

Figure 2. Cps 2-SO4, 6, and 7Bis do not decrease Jurkat cell growth. **A)** 10^5 Jurkat cells per mL were cultured in the presence of 100 µM of each compound or an equivalent volume of DMSO (control). An aliquot was taken at various times (1,2,3, and 6 days) and the Trypan blue-negative cell number evaluated and reported as the percentage of control cell value. The results shown are the average of three independent experiments. **B)**. 10^5 Jurkat cells per mL were seeded in a 96 well plate for 24 h before the addition of the Vibrant MTT reagent and measurement of metabolic proliferation by spectrometry. Results are reported as the percentage of the control value (cells grown in the presence of DMSO) and are the mean of three independent experiments. *p < 0.01, **p < 0.001, *** p < 0.0001, paired t-test.

Figure 3. Cp2-SO4 and Cp6 do not alter cell proliferation. A) 10^5 Jurkat cells and **B)** PBMC were labeled with Cell Proliferation Dye 670 (CPD) and grown for up to several days in complete medium containing DMSO or 100 µM Cp2-SO4 or Cp6. Cells were analyzed each day by flow cytometry. Representative histograms are shown. **C)** The proliferation index (left) and expansion index (right) were evaluated on day 3 for stimulated PBMC using the proliferation module of FlowJo.

Figure 4. Cp2-SO4, Cp6, and Cp7Bis do not induce apoptosis. Activated caspase 3 was measured by flow cytometry after exposition of cells to the compounds at 100 µM for 24h. **A & B)** Jurkat cells. **A)** Representative histograms. **B)** Mean of three independent experiments ± SEM. **C)** PBMC. Mean of three independent experiments ± SEM. *p < 0.01, **p < 0.001, *** p < 0.0001, paired t-test.

Figure 5. Cp2-SO4 reverses IL4I1-dependet inhibition of T-cell proliferation. 2 x 10^5 CPD Alexa Flour670-labeled PBMCs were incubated with 0.25 x 10^6 irradiated THP1 or THP1-IL4I1 cells in the presence of various concentrations of Cp2-S04 dissolved in DMSO (100, 200, or 400 µM). Control THP1 or THP1-IL4I1 were treated with equivalent volumes of DMSO. T cell proliferation was induced by the addition of anti-CD3 antibody and evaluated on day 5 by flow cytometry. **A)** Representative

histogram with Cp2-SO4 at 400 µM. **B)** Proliferation index, and **C)** expansion index. **B & C,** cumulative results from four independent experiments using cells of three different donors are shown as mean ± SEM. *p < 0.01, **p < 0.001, ***p < 0.0001, ****p < 0.00001, paired t-test.

10 BIBLIOGRAPHY

[1] V. Molinier-Frenkel, F. Castellano, Immunosuppressive enzymes in the tumor microenvironment, FEBS Lett 591(19) (2017) 3135-3157.

[2] A. Carbonnelle-Puscian, C. Copie-Bergman, M. Baia, N. Martin-Garcia, Y. Allory, C. Haioun, A. Cremades, I. Abd-Alsamad, J.P. Farcet, P. Gaulard, F. Castellano, V. Molinier-Frenkel, The novel immunosuppressive enzyme IL4I1 is expressed by neoplastic cells of several B-cell lymphomas and by tumor-associated macrophages, Leukemia 23(5) (2009) 952-60.

[3] F. Lasoudris, C. Cousin, A. Prevost-Blondel, N. Martin-Garcia, I. Abd-Alsamad, N. Ortonne, J.P. Farcet, F. Castellano, V. Molinier-Frenkel, IL4I1: an inhibitor of the CD8(+) antitumor T-cell response in vivo, Eur J Immunol 41(6) (2011) 1629-38.

[4] L. Bod, R. Lengagne, L. Wrobel, J.P. Ramspott, M. Kato, M.F. Avril, F. Castellano, V. Molinier-Frenkel, A. Prevost-Blondel, IL4-induced gene 1 promotes tumor growth by shaping the immune microenvironment in melanoma, Oncoimmunology 6(3) (2017) e1278331.

[5] J.P. Ramspott, F. Bekkat, L. Bod, M. Favier, B. Terris, A. Salomon, L. Djerroudi, K.S. Zaenker, Y. Richard, V. Molinier-Frenkel, F. Castellano, M.F. Avril, A. Prevost-Blondel, Emerging role of IL4-induced gene 1 as a prognostic biomarker affecting the local T cell response in human cutaneous melanoma, J Invest Dermatol (2018).

[6] P.J. Thul, L. Akesson, M. Wiking, D. Mahdessian, A. Geladaki, H. Ait Blal, T. Alm, A. Asplund, L. Bjork, L.M. Breckels, A. Backstrom, F. Danielsson, L. Fagerberg, J. Fall, L. Gatto, C. Gnann, S. Hober, M. Hjelmare, F. Johansson, S. Lee, C. Lindskog, J. Mulder, C.M. Mulvey, P. Nilsson, P. Oksvold, J. Rockberg, R. Schutten, J.M. Schwenk, A. Sivertsson, E. Sjostedt, M. Skogs, C. Stadler, D.P. Sullivan, H. Tegel, C. Winsnes, C. Zhang, M. Zwahlen, A. Mardinoglu, F. Ponten, K. von Feilitzen, K.S. Lilley, M. Uhlen, E. Lundberg, A subcellular map of the human proteome, Science 356(6340) (2017).

[7] M.F. Khirade, G. Lal, S.A. Bapat, Derivation of a fifteen gene prognostic panel for six cancers, Sci Rep 5 (2015) 13248.

[8] G. Finak, N. Bertos, F. Pepin, S. Sadekova, M. Souleimanova, H. Zhao, H. Chen, G. Omeroglu, S. Meterissian, A. Omeroglu, M. Hallett, M. Park, Stromal gene expression predicts clinical outcome in breast cancer, Nat Med 14(5) (2008) 518-27.

[9] F. Castellano, V. Molinier-Frenkel, IL4I1: An Emerging Target to Reinvigorate Antitumor Immune Responses, Immunotherapy: Open Access (2017).

[10] V. Molinier-Frenkel, A. Prevost-Blondel, F. Castellano, The IL4I1 Enzyme: A New Player in the Immunosuppressive Tumor Microenvironment, Cells 8(7) (2019).

[11] E. Le Gall, C. Haurena, S. Sengmany, T. Martens, M. Troupel, Three-component synthesis of alpha-branched amines under Barbier-like conditions, J Org Chem 74(20) (2009) 7970-3.

[12] C. Haurena, E. Le Gall, S. Sengmany, T. Martens, M. Troupel, A straightforward three-component synthesis of alpha-amino esters containing a phenylalanine or a phenylglycine scaffold, J Org Chem 75(8) (2010) 2645-50.

[13] J. Marquet, F. Lasoudris, C. Cousin, M. Puiffe, N. Martin-Garcia, V. Baud, F. Chéreau, J. Farcet, V. Molinier-Frenkel, F. Castellano, Dichotomy between factors inducing the immunosuppressive enzyme IL4I1 in B lymphocytes and mononuclear phagocytes, European Journal of Immunology 40 (2010) 2557-68.

[14] A. Carbonnelle-Puscian, C. Copie-Bergman, M. Baia, N. Martin-Garcia, Y. Allory, C. Haioun, A. Cremades, I. Abd-Alsamad, J.P. Farcet, P. Gaulard, F. Castellano, V. Molinier-Frenkel, The novel

immunosuppressive enzyme IL4I1 is expressed by neoplastic cells of several B-cell lymphomas and by tumor-associated macrophages, Leukemia 23(5) (2009) 952-960.
[15] S.S. Chavan, W. Tian, K. Hsueh, D. Jawaheer, P.K. Gregersen, C.C. Chu, Characterization of the human homolog of the IL-4 induced gene-1 (Fig1), Biochim Biophys Acta 1576(1-2) (2002) 70-80.
[16] C. Wang, F. Zhang, Y. Cao, M. Zhang, A. Wang, M. Xu, M. Su, M. Zhang, Y. Zhuge, Etoposide Induces Apoptosis in Activated Human Hepatic Stellate Cells via ER Stress, Sci Rep 6 (2016) 34330.
[17] F. Castellano, V. Molinier-Frenkel, An Overview of l-Amino Acid Oxidase Functions from Bacteria to Mammals: Focus on the Immunoregulatory Phenylalanine Oxidase IL4I1, Molecules 22(12) (2017).
[18] I.M. Moustafa, S. Foster, A.Y. Lyubimov, A. Vrielink, Crystal structure of LAAO from Calloselasma rhodostoma with an L-phenylalanine substrate: insights into structure and mechanism, Journal of Molecular Biology 364(5) (2006) 991-1002.
[19] Y. He, E. Orton, D. Yang, The Selection of a Pharmaceutical Salt-The Effect of the Acidity of the Counterion on Its Solubility and Potential Biopharmaceutical Performance, J Pharm Sci 107(1) (2018) 419-425.
[20] P.D. Pawelek, J. Cheah, R. Coulombe, P. Macheroux, S. Ghisla, A. Vrielink, The structure of L-amino acid oxidase reveals the substrate trajectory into an enantiomerically conserved active site, Embo J 19(16) (2000) 4204-15.

11 GLOSSARY

IL4I1 Interleukin-induced gene 1
PBMC Periferal Blood Mononuclear Cells

Figure 1

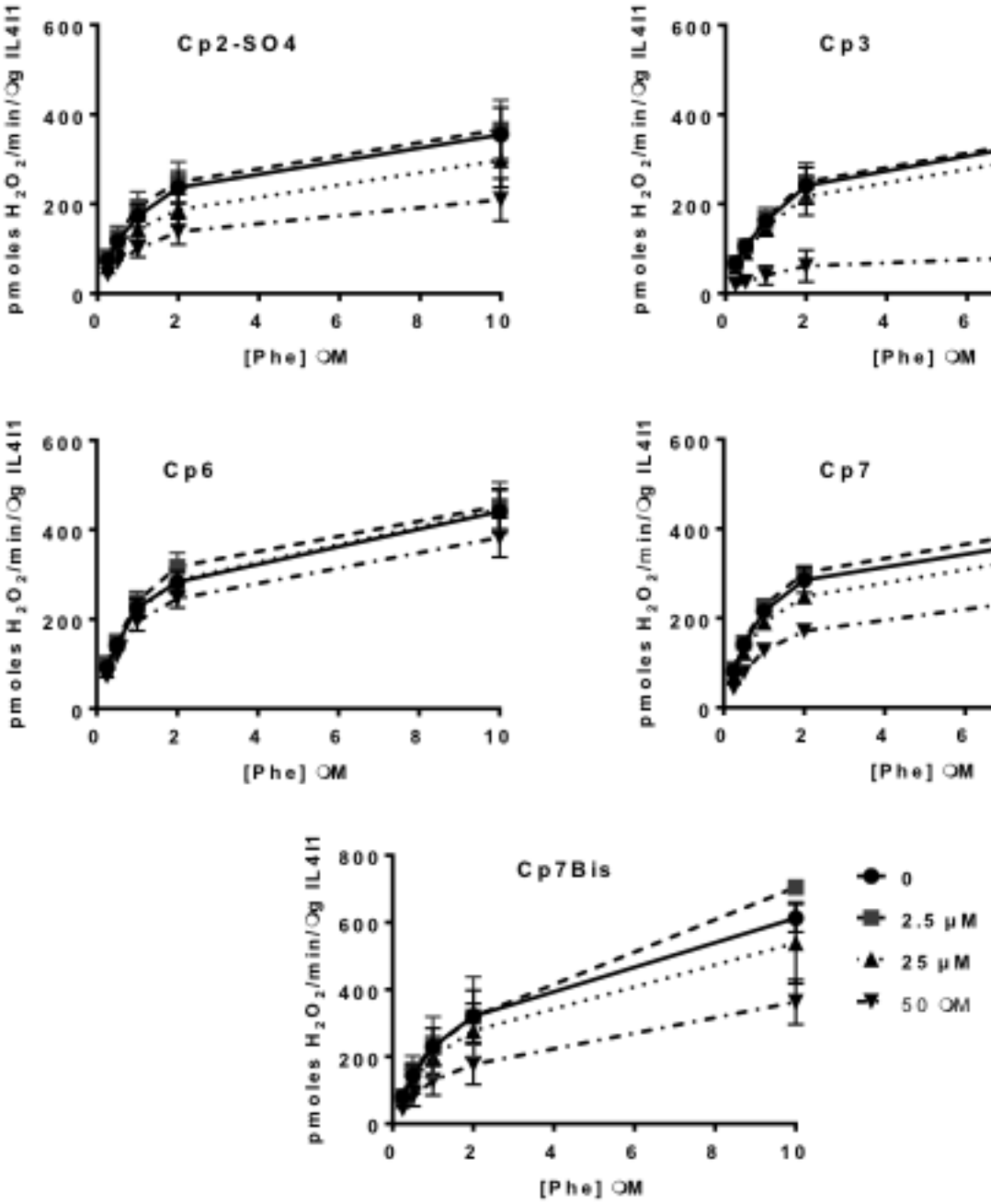
Cp2-SO4
Cp3
Cp6
Cp7
Cp7Bis
pmoles H2O2/min/µg IL4I1
[Phe] µM
0
2.5 µM
25 µM
50 µM

Figure 2

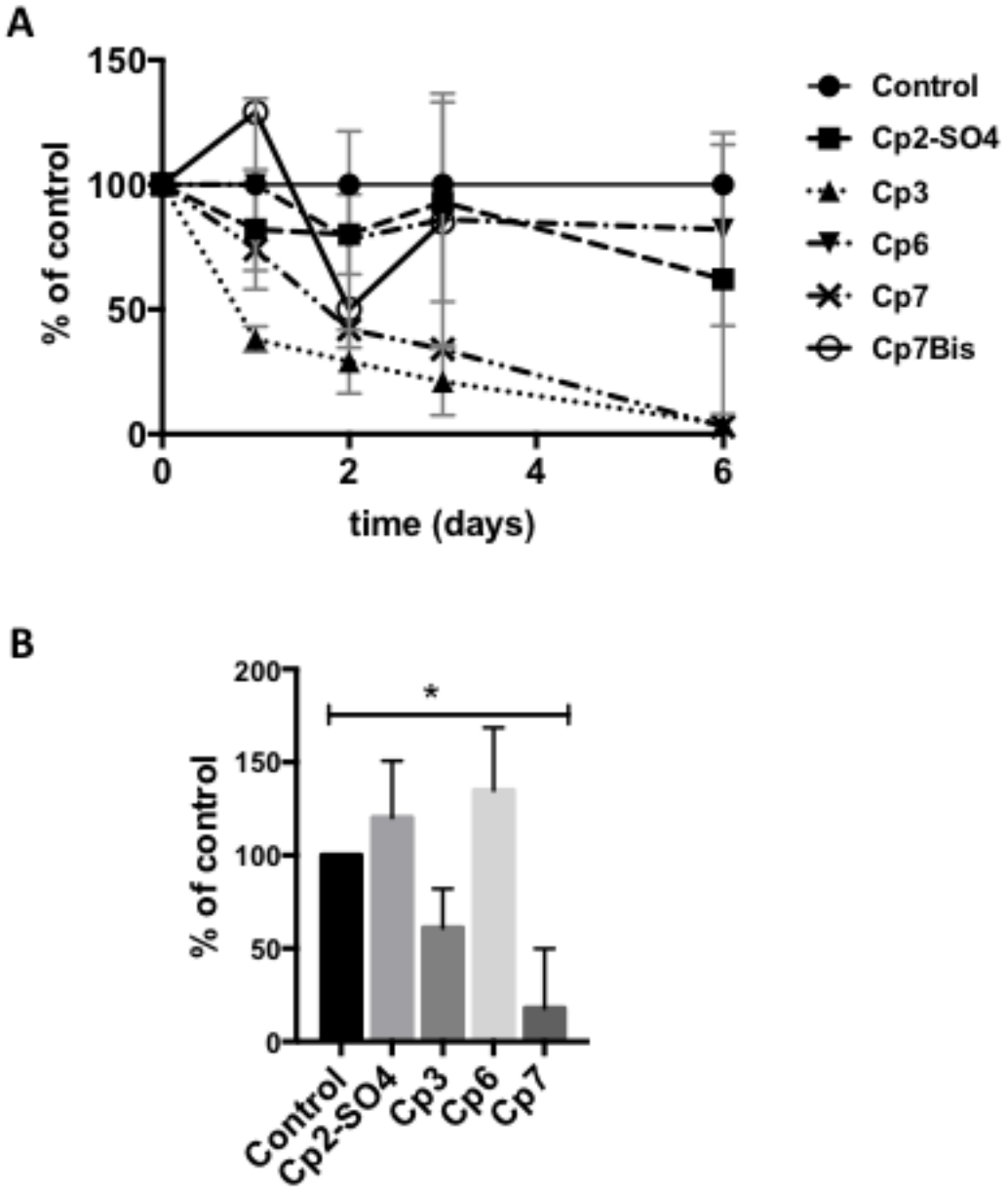
A
150
100
50
0
% of control
0
2
4
6
time (days)
Control
Cp2-SO4
Cp3
Cp6
Cp7
Cp7Bis
B
200
150
100
50
0
% of control
*
Control
Cp2-SO4
Cp3
Cp6
Cp7

Figure 3

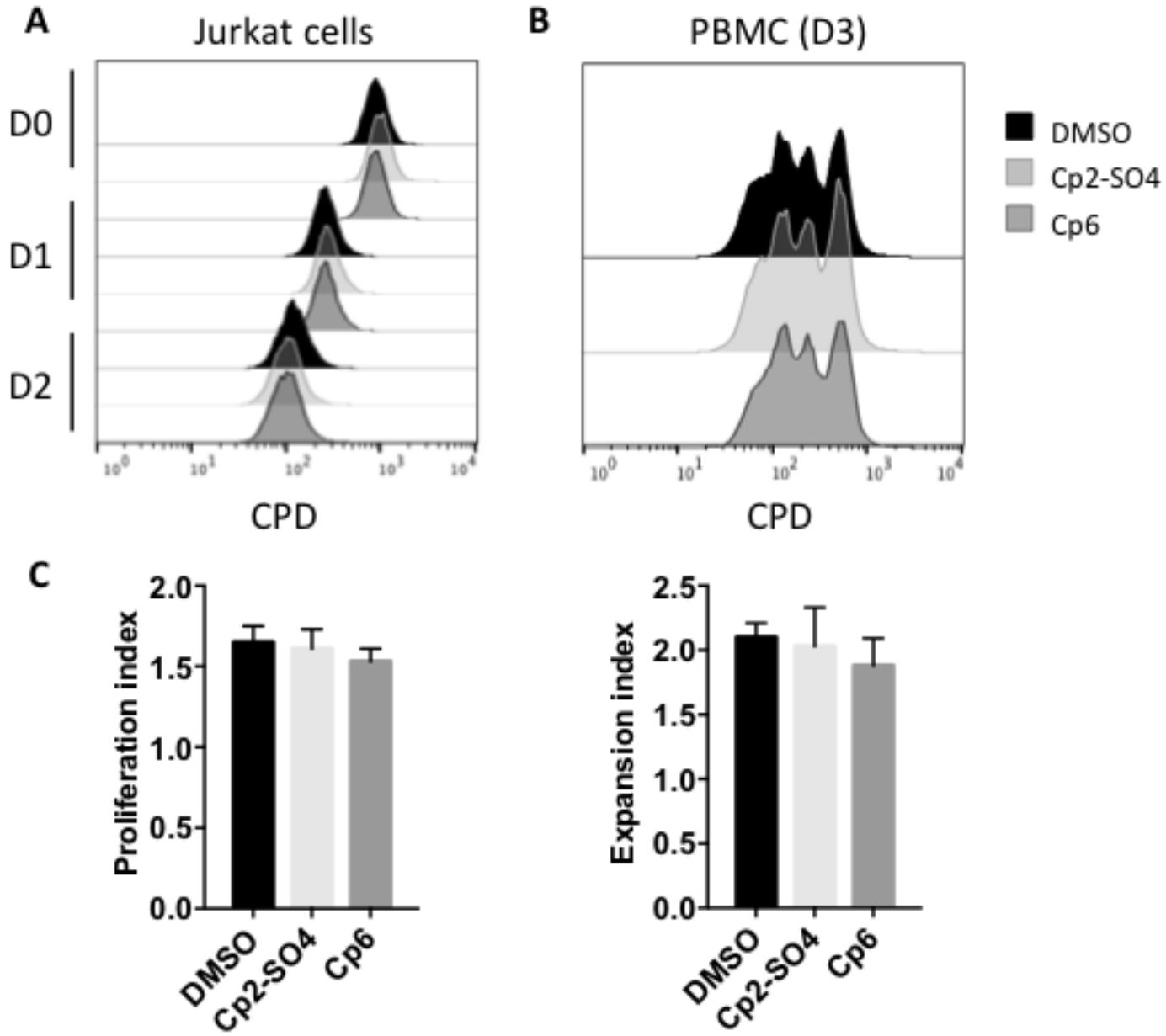
A
Jurkat cells
D0
D1
D2
CPD
B
PBMC (D3)
CPD
DMSO
Cp2-SO4
Cp6
C
Proliferation index
2.0
1.5
1.0
0.5
0.0
DMSO
Cp2-SO4
Cp6
Expansion index
2.5
2.0
1.5
1.0
0.5
0.0
DMSO
Cp2-SO4
Cp6

Figure 4

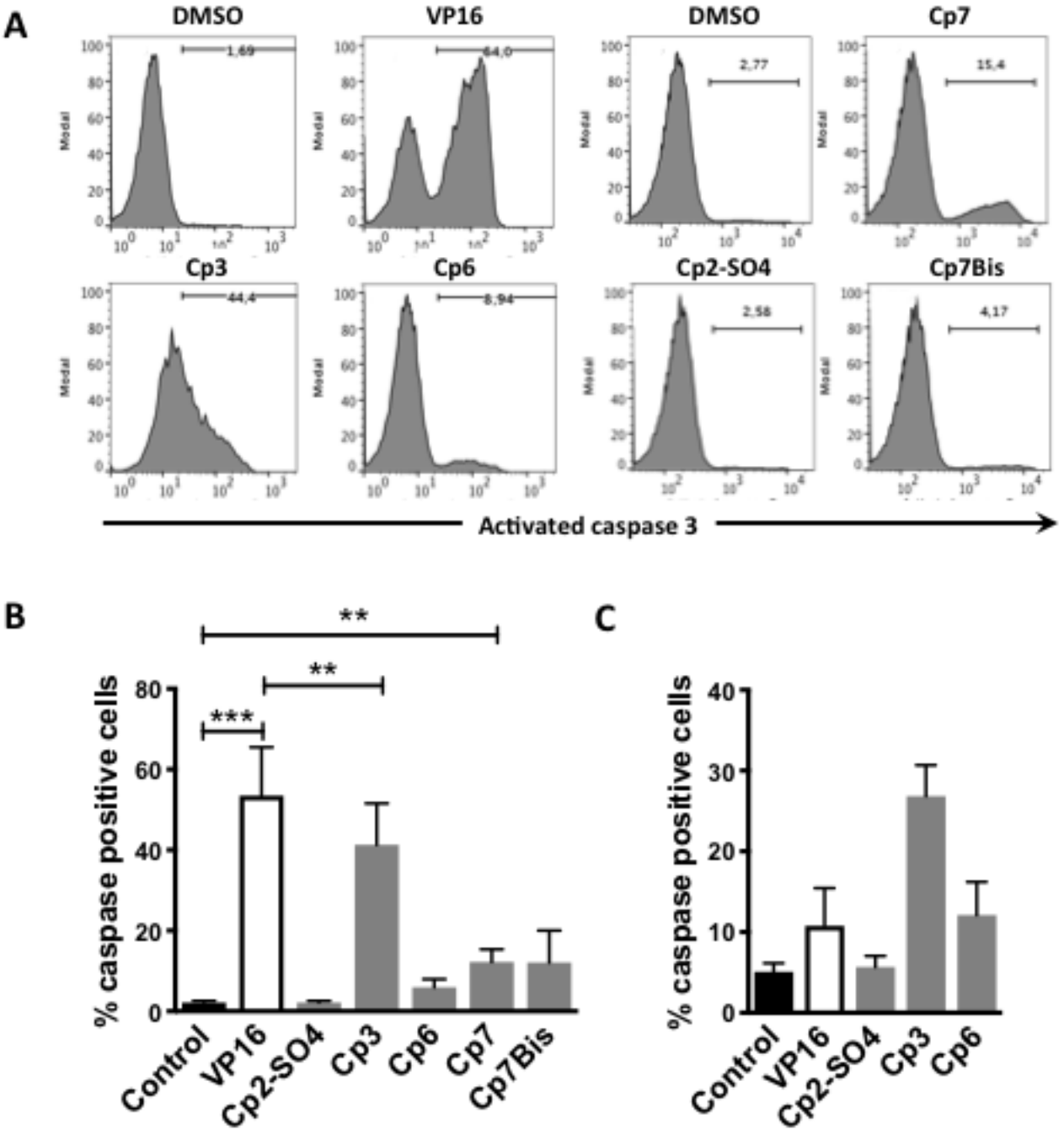
A
DMSO
VP16
DMSO
Cp7
Cp3
Cp6
Cp2-SO4
Cp7Bis
1,69
64,0
2,77
15,4
44,4
8,94
2,58
4,17
Modal
Activated caspase 3
B
% caspase positive cells
**
**
***
Control
VP16
Cp2-SO4
Cp3
Cp6
Cp7
Cp7Bis
C
% caspase positive cells
Control
VP16
Cp2-SO4
Cp3
Cp6

Figure 5

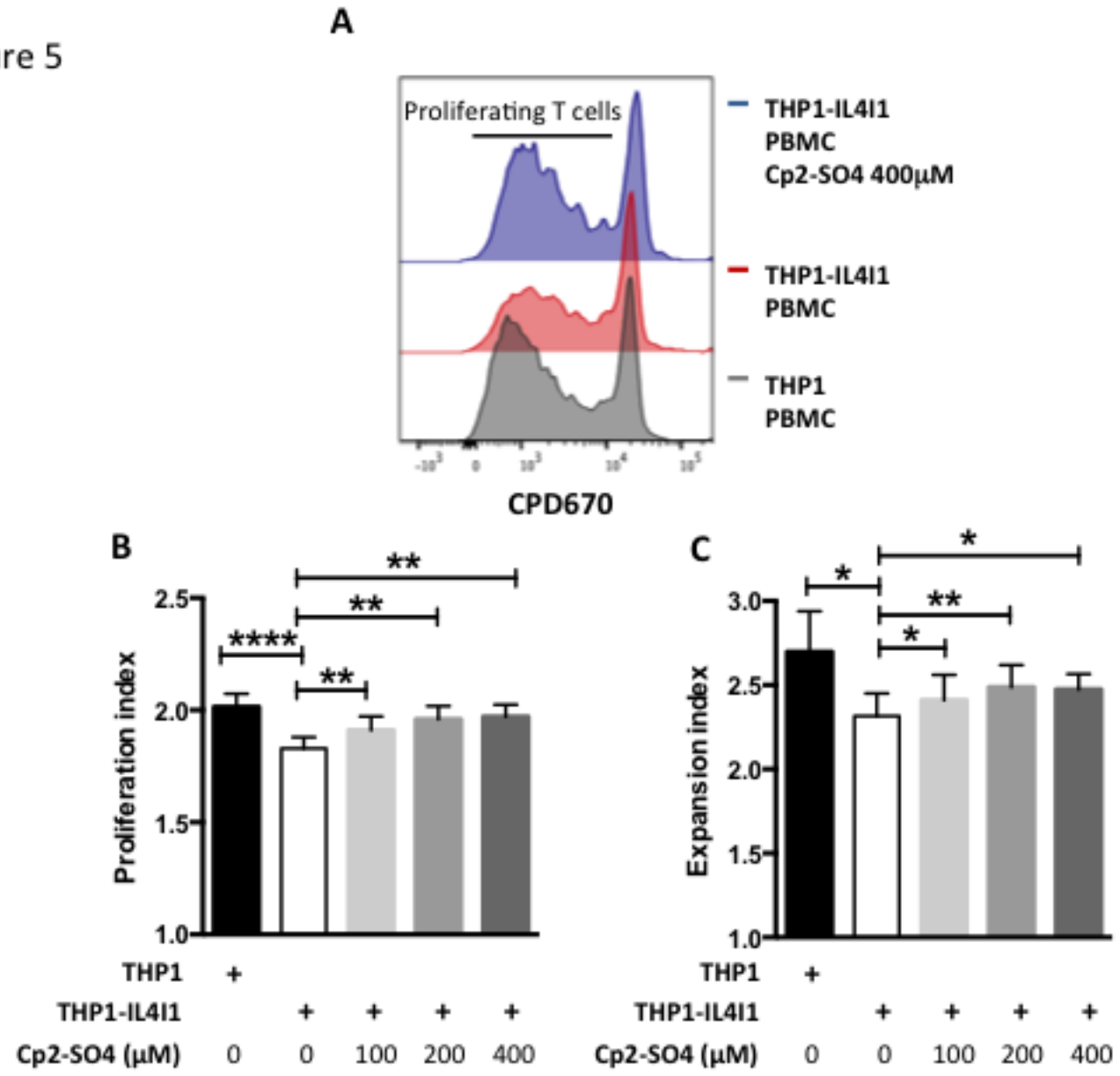
A
Proliferating T cells
THP1-IL4I1
PBMC
Cp2-SO4 400µM
THP1-IL4I1
PBMC
THP1
PBMC
CPD670
B
Proliferation index
2.5
2.0
1.5
1.0
****
**
**
**
THP1 +
THP1-IL4I1 + + + +
Cp2-SO4 (µM) 0 0 100 200 400
C
Expansion index
3.0
2.5
2.0
1.5
1.0
*
*
**
*
THP1 +
THP1-IL4I1 + + + +
Cp2-SO4 (µM) 0 0 100 200 400

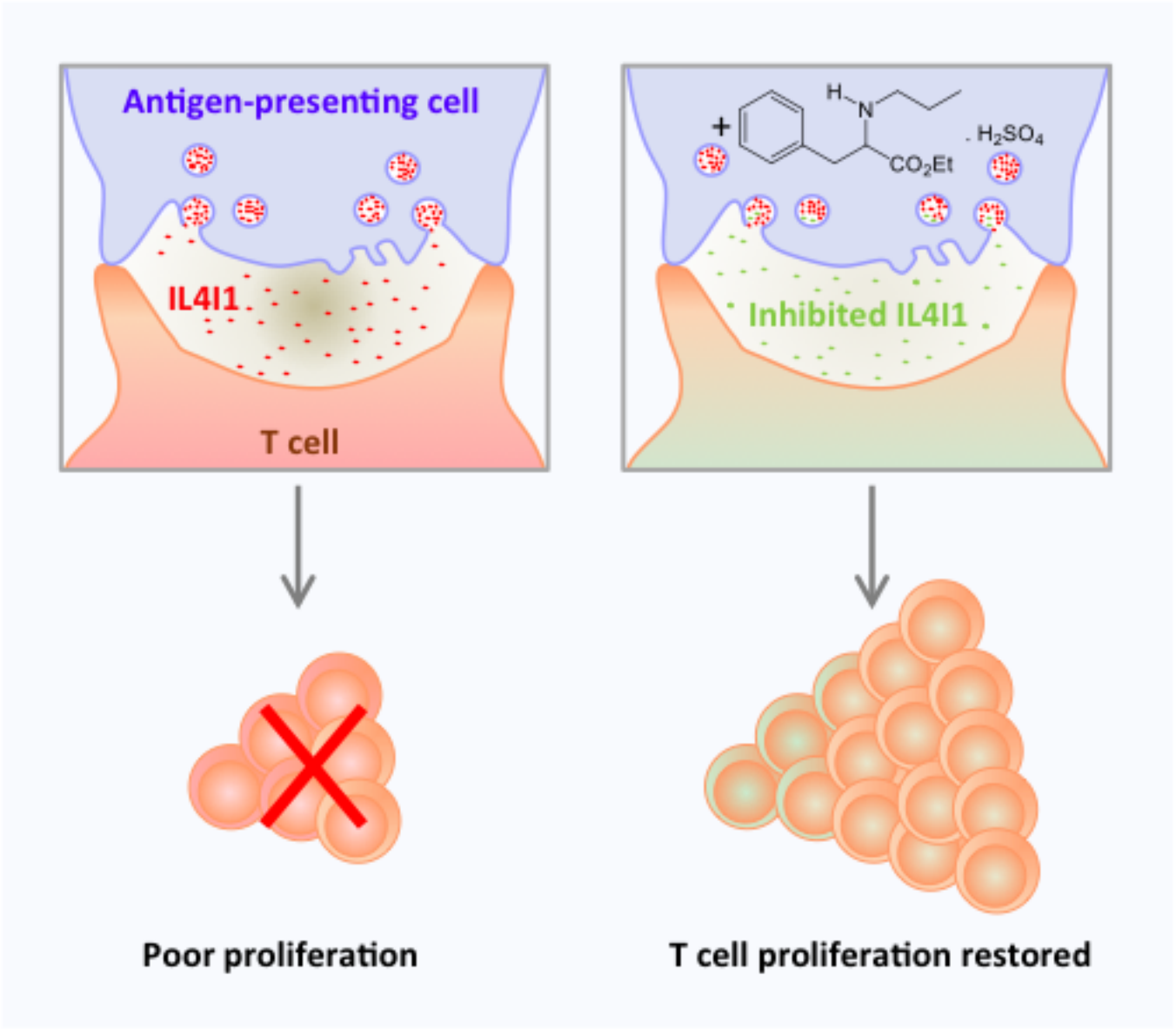
Antigen-presenting cell
IL4I1
T cell
Inhibited IL4I1
Poor proliferation
T cell proliferation restored